

**Supporting Information for**  
**Intrinsic Ferromagnetism in 2D *h*-CrC Semiconductor with Strong**  
**Magnetic Anisotropy and High Curie Temperature**

Kang Sheng, Hong-Kuan Yuan, and Zhi-Yong Wang\*

*School of Physical Science and Technology,*  
*Southwest University, Chongqing 400715, China*

---

\* Corresponding author: zywang@swu.edu.cn (Z.-Y. Wang)

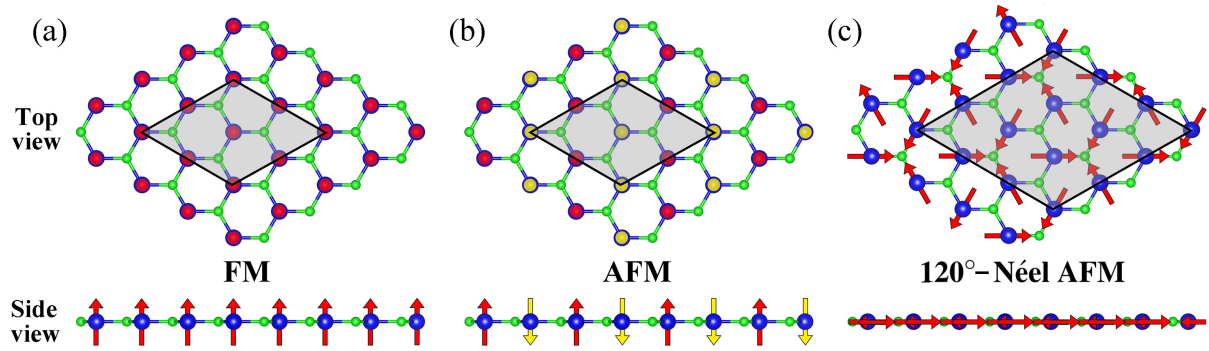


FIG. S1: Top and side views of (a) FM, (b) AFM, and (c) 120°-Néel AFM configurations of 2D  $h$ -CrC crystal. A  $2 \times 2 \times 1$  supercell is used to simulate the collinear FM and AFM spin configurations, while a  $3 \times 3 \times 1$  supercell is considered for the noncollinear 120°-Néel AFM configuration. Our calculations show that the energy of the FM configuration are lower than those of the AFM and 120°-Néel AFM configurations by 0.31 and 0.37 eV per Cr atom, respectively.

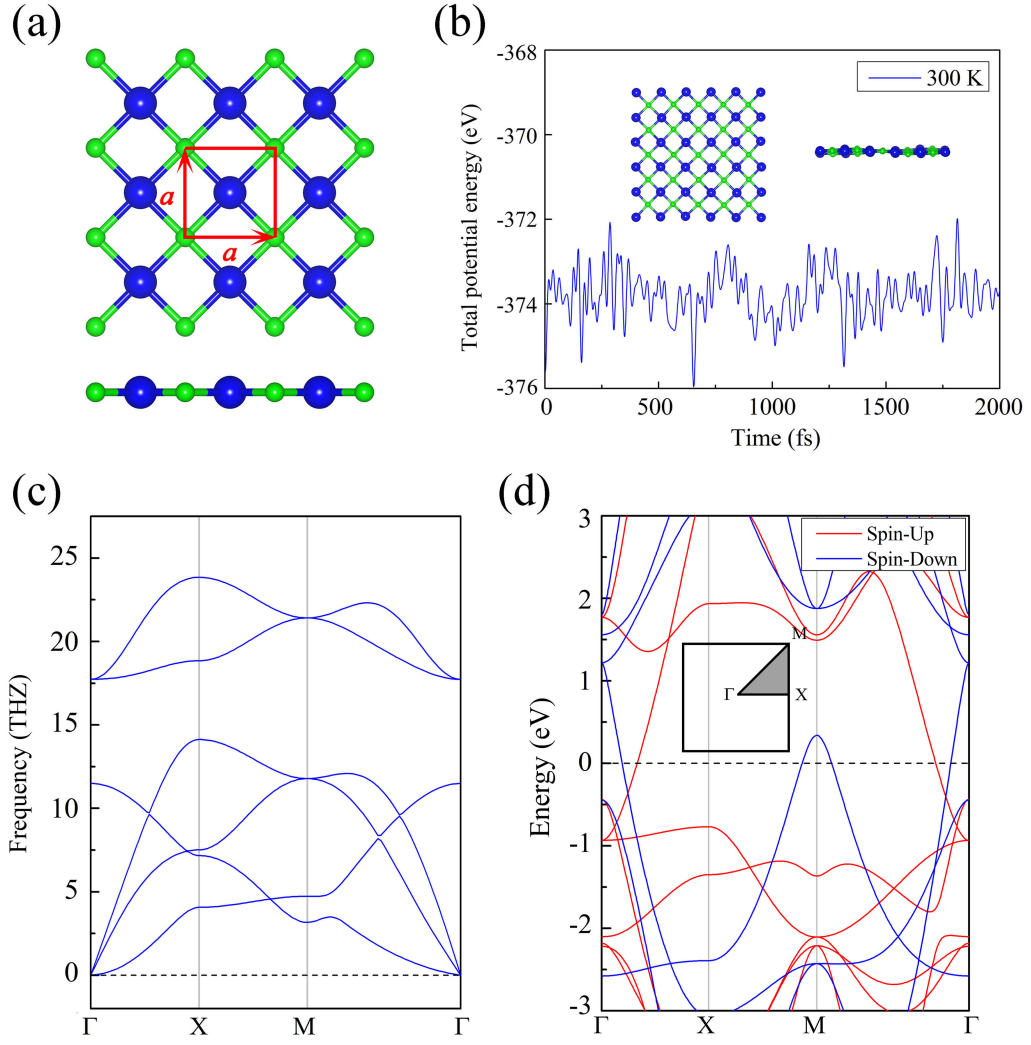


FIG. S2: Information of the *t*-CrC monolayer that is associated with the (100) plane of the rock-salt bulk CrC crystal. (a) Top and side views of the crystal structure with an equilibrium lattice constant of 2.79 Å. (b) Small fluctuation of total energy during AIMD simulations at 300 K and the integrity of the original configuration at 2 ps confirm excellent thermal stability of the *t*-CrC monolayer. (c) The phonon dispersions of the *t*-CrC monolayer reveal the absence of imaginary modes in the whole Brillouin zone, establishing its dynamic stability. (d) The calculated band structure at the GGA+*U* level indicates that the *t*-CrC monolayer is a magnetic metal.

TABLE S1: Comparison of structural information of both  $t$ -CrC and  $h$ -CrC monolayers, which covers the equilibrium lattice constant ( $a$ ), the Cr-C distance ( $d$ ), the cohesive energy ( $E_{\text{coh}}$ ), the magnetic moment per unit cell ( $M$ ), and space group.

Structure	$a$ (Å)	$d$ (Å)	$E_{\text{coh}}$ (eV)	$M$ ( $\mu_B$ )	Space group
$t$ -CrC	2.79	1.98	4.42	2.11	$P4/mmm$
$h$ -CrC	3.27	1.89	3.93	2.00	$P\bar{6}m2$

\* In view of the fact that the unit cell of the  $t$ -CrC monolayer consists of one Cr atom and one C atom, the cohesive energy is therefore calculated via the same formula as the  $h$ -CrC monolayer.

TABLE S2: Summary of all kinds of calculated data for the FM  $\text{CrX}_3$  ( $X = \text{Cl}, \text{Br}, \text{and I}$ ) monolayers, which involve the equilibrium lattice constant ( $a$ ), the magnetic moment ( $M$ ) per Cr atom, the exchange energy ( $E_{\text{ex}} = E_{\text{AFM}} - E_{\text{FM}}$ ) per unit cell, the magnetic anisotropic energy ( $\text{MAE} = E_{\text{in-plane}} - E_{\text{out-of-plane}}$ ) per Cr atom, the nearest-neighboring exchange constant ( $J$ ), the single site magnetic anisotropy parameter ( $A$ ) and the Curie temperature from Monte Carlo simulations based on the classical Heisenberg model ( $T_{\text{C}}^{\text{MC}}$ ). Also, the experimentally measured Curie temperatures ( $T_{\text{C}}^{\text{EXP}}$ ) are provided for comparison.

Monolayer	$a$ (Å)	$M$ ( $\mu_B$ )	$E_{\text{ex}}$ (eV)	MAE ( $\mu\text{eV}$ )	$J$ (meV)	$A$ ( $\mu\text{eV}$ )	$T_{\text{C}}^{\text{MC}}$ (K)	$T_{\text{C}}^{\text{EXP}}$ (K)
$\text{CrCl}_3$	6.12	3.0	0.029	30	0.537	3.33	11	17
$\text{CrBr}_3$	6.51	3.0	0.038	166	0.704	18.44	22	27
$\text{CrI}_3$	7.08	3.0	0.049	768	0.907	85.33	43	45

\* To evaluate  $T_{\text{C}}^{\text{MC}}$ , we make use of  $E_{\text{ex}} = 6J|S|^2$  and  $A = \text{MAE}/|S|^2$  with  $|S|$  equal to 3.0. Clearly, our simulated  $T_{\text{C}}^{\text{MC}}$  is consistent with the experimentally measured  $T_{\text{C}}^{\text{EXP}}$  for all of three  $\text{CrX}_3$  monolayers.

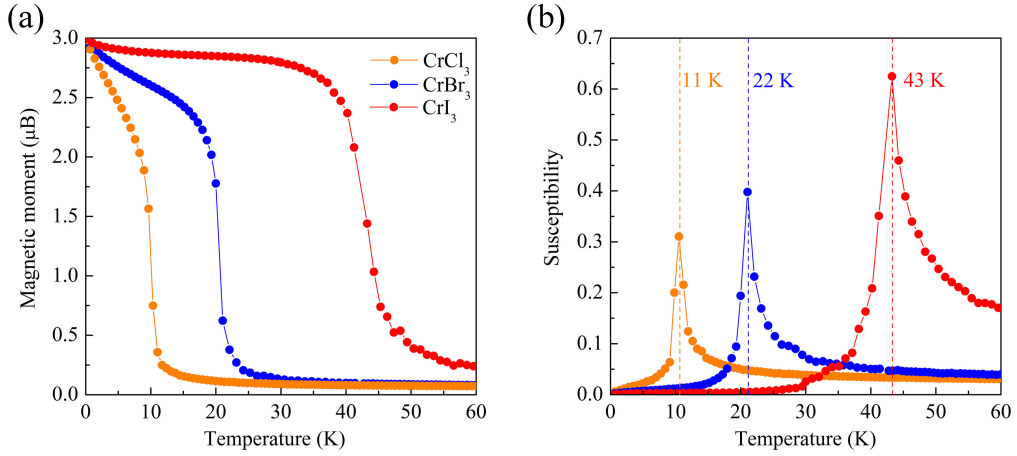


FIG. S3: Simulated magnetic moment per unit cell and magnetic susceptibility with respect to temperature for the  $\text{CrCl}_3$ ,  $\text{CrBr}_3$ , and  $\text{CrI}_3$  monolayers, respectively.

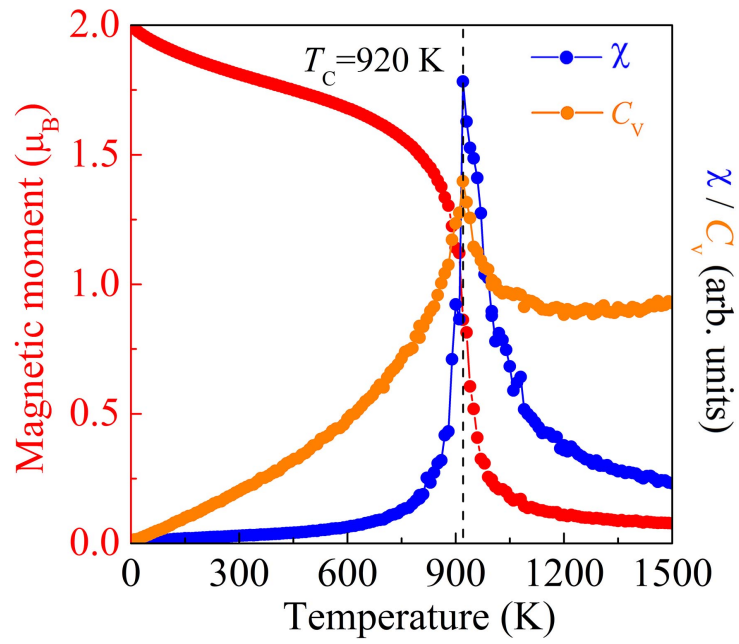


FIG. S4: Average magnetic moment (red curve) per unit cell, specific heat  $C_v$  (orange curve), and magnetic susceptibility  $\chi$  (blue curve) versus temperature from MC simulations for 2D  $h$ -CrC crystal with  $J = 26.43$  meV and  $A = 56.19 \mu\text{eV}$  obtained at the HSE06 level. The Curie temperature is predicted to be 920 K.

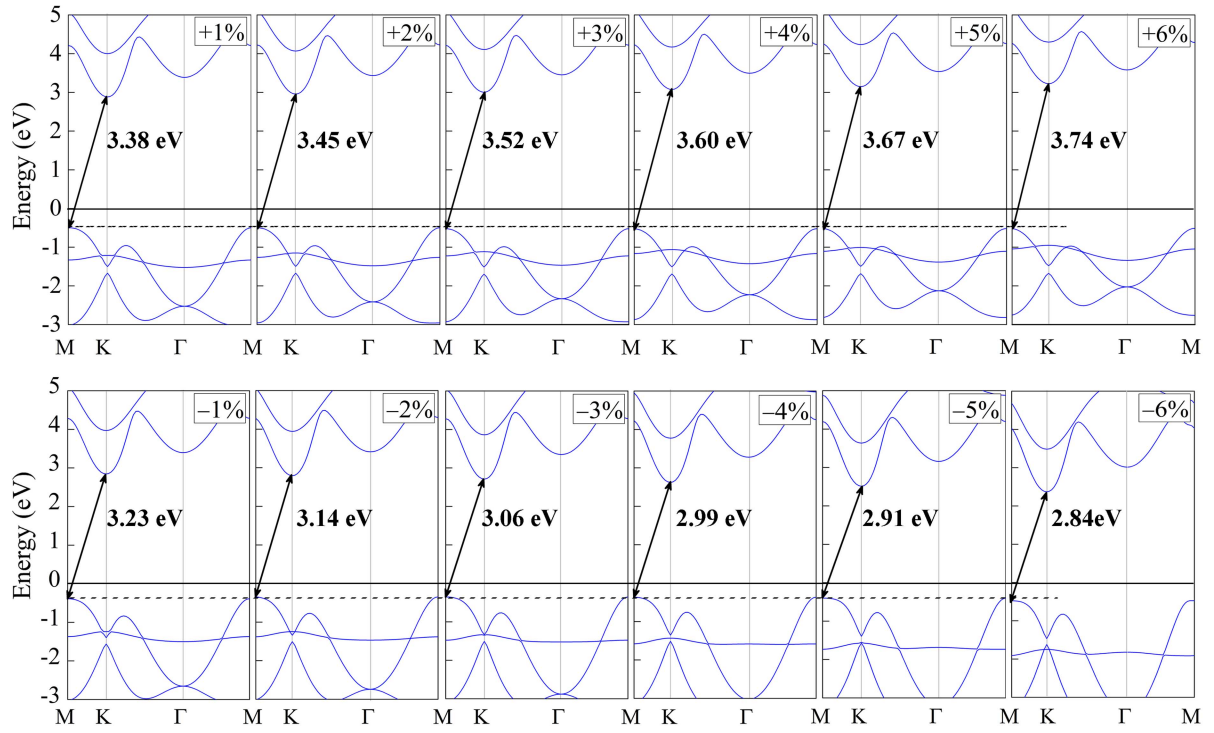


FIG. S5: Spin-polarized band structures of the *h*-CrC monolayer at the HSE06 level under different biaxial strains for the spin-down channel. The Fermi level is set to zero and indicated by the black solid line.

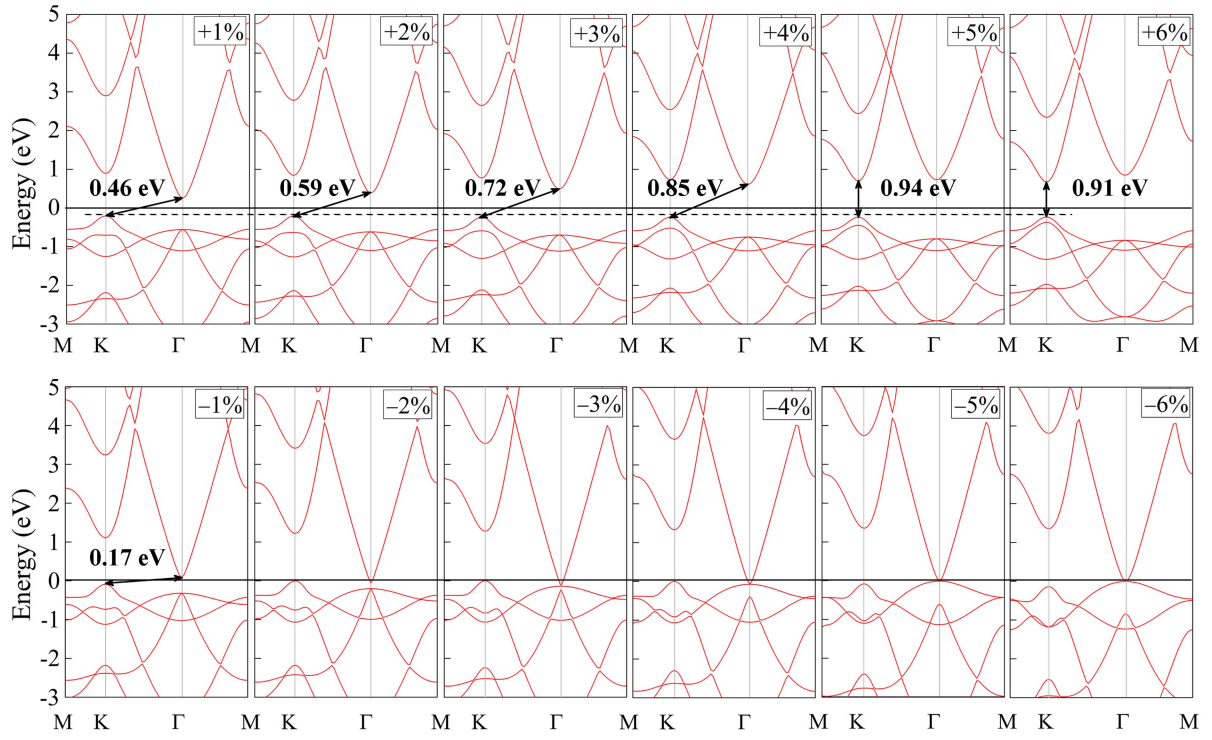


FIG. S6: Spin-polarized band structures of the  $h$ -CrC monolayer at the HSE06 level under different biaxial strains for the spin-up channel. The Fermi level is set to zero and indicated by the black solid line.

TABLE S3: Summary of all kinds of calculated data under different levels of biaxial strain for the  $h$ -CrC monolayer, which include the exchange energy ( $E_{\text{ex}} = E_{\text{AFM}} - E_{\text{FM}}$ ) per unit cell, the magnetic anisotropic energy (MAE =  $E_{\text{in-plane}} - E_{\text{out-of-plane}}$ ), the nearest-neighboring exchange constant ( $J$ ), the single site magnetic anisotropy parameter ( $A$ ), and the Curie temperature ( $T_C$ ) from Monte Carlo simulations.

Stain (%)	$E_{\text{ex}}$ (eV)	MAE ( $\mu\text{eV}$ )	$J$ (meV)	$A$ ( $\mu\text{eV}$ )	$T_C$ (K)
6	0.260	262	16.22	65.50	605
5	0.268	248	16.73	62.00	610
4	0.276	236	17.22	59.00	622
3	0.283	211	17.70	52.75	590
2	0.291	167	18.19	41.75	560
1	0.299	117	18.69	29.25	520
0	0.306	138	19.14	34.50	555
-1	0.314	178	19.61	44.50	641
-2	0.320	230	20.03	57.50	718
-3	0.327	536	20.41	134.00	979
-4	0.332	587	20.73	146.75	1038
-5	0.335	623	20.95	155.75	1035
-6	0.338	669	21.11	167.25	1077

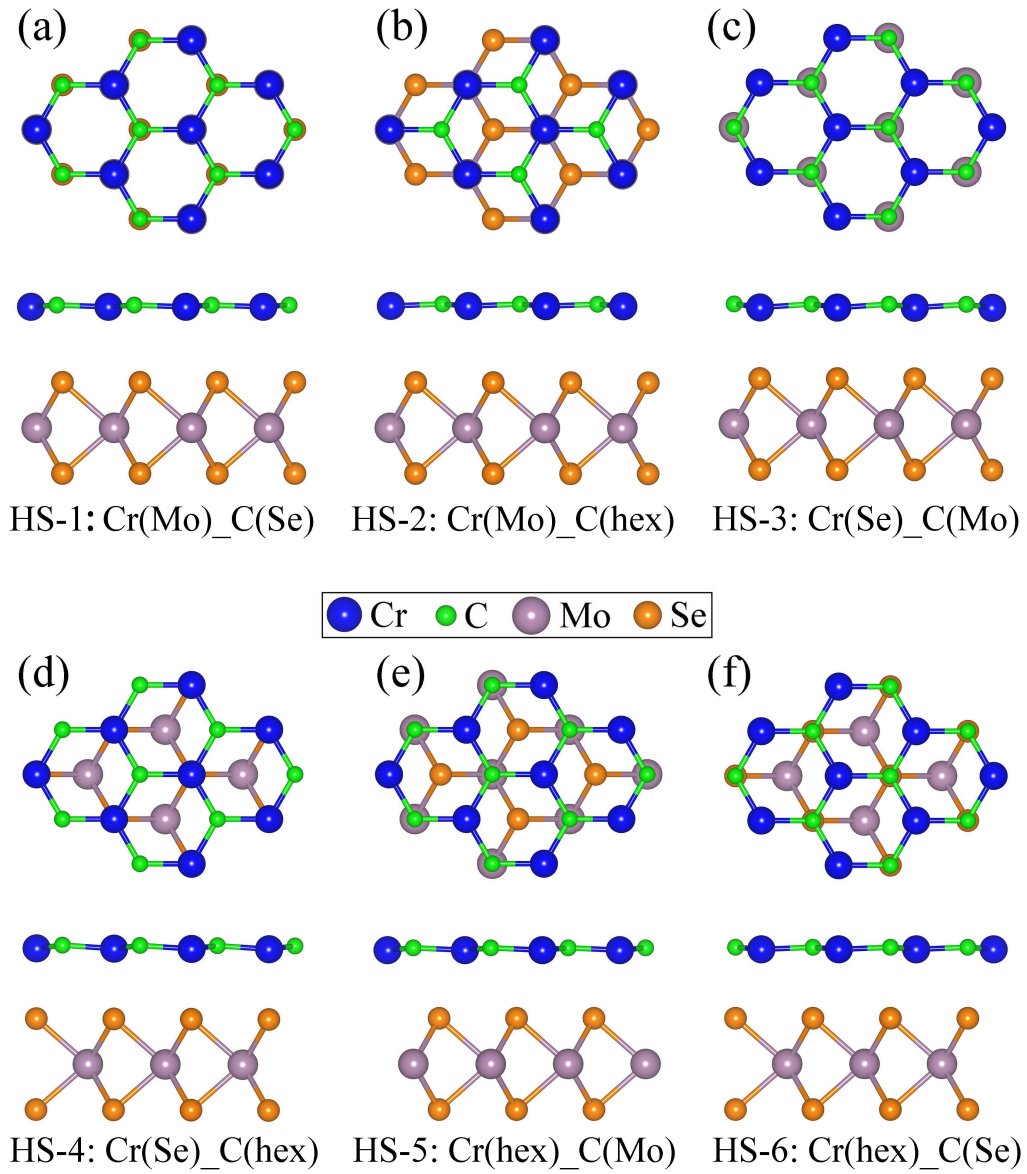


FIG. S7: Top and side views of six possible configurations of the  $h$ -CrC/MoSe<sub>2</sub> heterostructures by means of different arrangements of the  $h$ -CrC monolayer on the top of the MoSe<sub>2</sub> substrate. Here the coordination partners of both Cr and C atoms are presented in parentheses and the coordination pairs are separated by underscores. The symbol (hex) denotes the position of either Cr or C atoms directly above the centers of MoSe<sub>2</sub> hexagons.

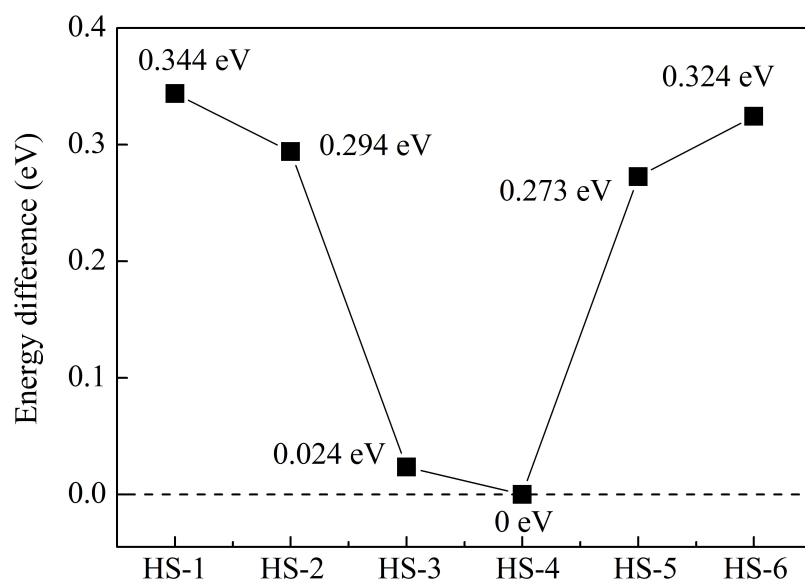


FIG. S8: Energies of six possible heterostructures in their equilibrated states against the most energetically stable HS-4 configuration. Note that since there remains only minor energy difference (0.024 eV) between the HS-3 and HS-4 configurations, both of them may be realized experimentally.

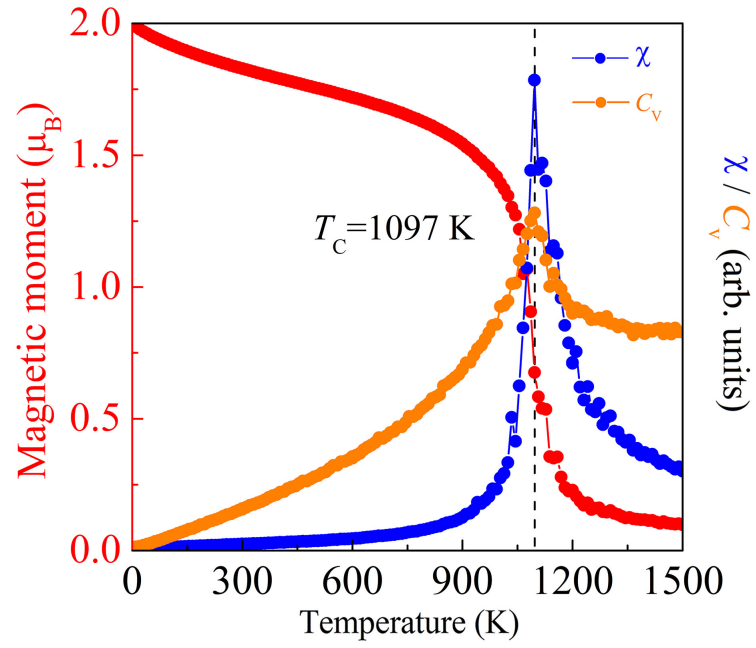


FIG. S9: Average magnetic moment (red curve) per unit cell, specific heat  $C_V$  (orange curve), and magnetic susceptibility  $\chi$  (blue curve) versus temperature from MC simulations for the  $h$ -CrC/MoSe<sub>2</sub> heterostructure with  $J = 31.91$  meV and  $A = 53.09$   $\mu$ eV obtained at the GGA+ $U$  level. The Curie temperature is predicted to be 1097 K.